博士論文（要約）

Critical role of genomic enhancer in converting TCR signal to apoptosis in thymic negative selection

（胸腺ネガティブ選択において TCR シグナルをアポトーシスに導く
エンハンサーの同定と解析）

荒井　未来

Contents

本博士論文中 1 ページ目から 96 ページ目については，単行本もしくは雑誌掲載等の形で刊行される予定（5 年以内に出版予定）であるため，以下に内容を要約したものを示す.

【研究背景】

T 細胞は獲得免疫の中心を担う細胞である．それぞれの T 細胞は，細胞ごとに異なる 1 種類の T 細胞受容体（T cell receptor；TCR）をその表面に発現しており，TCR によって異物を認識する. T 細胞は胸腺で分化するが, その際, 遺伝子再構成によって膨大な TCR レパートリーがつくられる(Klein et al., 2014)．これによって，生体は未知の病原体をも排除可能としている．しかし，出来上がった TCR の中には自己を認識するものも含まれる．この自己応答性 T 細胞を排除するため，T 細胞は分化の際，ネガティブセレクションとよばれる過程を経験する．ネガティブセレクションでは，出来上がった TCR に対して，主要組織適合遺伝子複合体（major histocompatibility complex；MHC）に自己抗原（self-peptide）がのったもの（self-pMHC）が提示される(Klein et al., 2014)．Self-pMHC に高い親和性を示す TCR を発現する T 細胞は自己応答性とみなされ，アポトーシスによって排除される(Klein et al., 2014)．ネガティブセレクションにはアポトーシス促進遺伝子 *Bim* が必須であることが過去の研究から示されている(Bouillet et al., 2002; Labi et al., 2014)．しかし，self-pMHC との結合による TCR 刺激がどのように *Bim* へと伝わるのかについては，不明な点が多い．また *Bim* はネガティブセレクション以外にも，発生過程における四肢の水かきの消滅, 抹消での免疫機能の恒常性維持など様々な過程で働くユビキタスな遺伝子である(Bouillet et al., 2002; Labi et al., 2014)．その *Bim* が胸腺におけるネガティブセレクション時にどのような制御を受けているのかも不明である.

本研究では上記の問いに答えるため，エンハンサーに着目した．エンハンサーとは細胞種及びシグナル依存的な遺伝子の発現を規定するゲノム領域である(Calo and

Wysocka, 2013). 我々は，*Bim* 近傍に胸腺で特異性の高いエンハンサー領域，E^{BAB} を同定した．E^{BAB} ノックアウトマウス（ΔE^{BAB} マウス）の胸腺細胞は，TCR シグナルによって誘導されるアポトーシス及び *Bim* の発現に不全を示した．しかし，ΔE^{BAB} マウスは抹消及び制御性 T 細胞の恒常性に異常を示さなかった．したがって E^{BAB} は，胸腺ネガティブセレクション特異的に *Bim* の発現を制御しているエンハンサー領域であることが示された．

【結果・考察】

ΔE^{BAB} 胸腺には high affinity TCR clone が蓄積する

我々はまず公共の ChIP-seq データを用いて，H3K27ac^{high} かつ H3K4me3^{low} であるエンハンサー候補領域(Calo and Wysocka, 2013) を探索し，*Bim* 近傍に胸腺で特異性の高いエンハンサー候補領域を発見した．これを E^{BAB} と名づけ，E^{BAB} の生理的機能を明らかにすべく，E^{BAB} ノックアウトマウス（ΔE^{BAB} マウス）を作成した．

まずΔE^{BAB} 胸腺細胞を anti-CD4 抗体及び anti-CD8 抗体で染色し，E^{BAB} の T 細胞分化過程に対する影響を調べた．ΔE^{BAB} マウスでは CD4/CD8 の分布に変化がみられ，double negative（DN），CD4 single positive（CD4 SP），CD8 SP の割合が増加，double positive（DP）の割合が減少していた．その原因を探るため，胸腺細胞の RNA-seq を行った．その結果，自己抗原に対して高い親和性を示す TCR を発現しているクローン（high affinity TCR clone）に特徴的な遺伝子の発現が上昇していた．そこで，胸腺細胞を anti-TCRβ抗体及び anti-CD69 抗体で染色し，ΔE^{BAB} 胸腺における high affinity TCR clone の蓄積を調べた．ΔE^{BAB} 胸腺では，TCRβ^{high}/CD69^{high} 集団の割合が上昇している様子が観察されたことから，high affinity TCR clone が蓄積していると考えられた．

ΔE^{BAB} 胸腺細胞は TCR シグナル依存的なアポトーシスの不全を起こす

ΔE^{BAB} 胸腺において high affinity TCR clone が蓄積することから，我々は，ΔE^{BAB} マウスがネガティブセレクションにおけるアポトーシスに異常をきたしているという仮説を立てた．まず野生型（WT）およびΔE^{BAB} 胸腺細胞に anti-CD3 抗体及び anti-CD28 抗体を処理することで ex vivo でネガティブセレクション過程を模し，その際のアポトーシス細胞の割合を AnnexinV/PI 染色により計測した．ΔE^{BAB} では WT と比較して，TCR シグナル依存的な初期アポトーシス細胞（Annexin V^+/PI^-）の割合が減少していた．

次に，OT-II transgenic system（OT-II tg）を用い，上記の仮説を in vivo で検証した．OT-II tg マウスの T 細胞は，chicken ovalbumin 323-339 残基（$OVA_{323-339}$）を認識する TCR を発現している(Barnden et al., 1998; Bouillet et al., 2002)．我々は，WT ; OT-II tg, $E^{BAB+/-}$; OT-II tg，ΔE^{BAB} ; OT-II tg マウスを作成し，それぞれに $OVA_{323-339}$ 及びコントロールとして $OVA_{257-264}$ を腹腔内投与し，72 時間後の胸腺細胞の様子を anti-CD4/CD8 抗体染色によって調べた．WT ; OT-II tg，$E^{BAB+/-}$; OT-II tg では，$OVA_{323-339}$ の腹腔内投与によって，CD4 SP の割合の顕著な減少が観察された．この減少は，ΔE^{BAB} ; OT-II tg ではレスキューされていた．以上の結果から，E^{BAB} はネガティブセレクションにおける high affinity TCR clone の除去に必須であると考えられた．

E^{BAB} は TCR シグナル依存的な *Bim* の発現に必須である

次に我々は，ΔE^{BAB} 胸腺細胞の TCR シグナル依存的なアポトーシス不全が，E^{BAB} 近傍のアポトーシス促進遺伝子 *Bim* の発現異常によるものであるという仮説を立てた．まず，WT 及びΔE^{BAB} 胸腺細胞に anti-CD3/CD28 抗体で刺激を与え, その際の *Bim* の発現を qRT-PCR によって調べた．WT と比較してΔE^{BAB} では，刺激による *Bim* の発現上昇の程度は低かった．このとき，TCR シグナル強度のマーカー遺伝子である *Nr4a1* の発現は，WT とΔE^{BAB} とで同程度であった．

次に，TCR シグナル依存的な *Bim* の発現をより生理的な条件で調べるために，

TCRβ^{high}/CD69^{high}胸腺細胞（TCR activated）と TCRβ^{low}/CD69^{low}胸腺細胞（TCR inactivated）とをセルソーターで分け，それぞれにおける *Bim* の発現を測定した．TCRβ^{high}/CD69^{high}におけるΔE^{BAB} の *Bim* の発現は WT と比較して低かった．TCR^{low}/CD69^{low}においてもΔE^{BAB} の *Bim* の発現は WT と比較して低い傾向であったものの，TCRb^{high}/CD69^{high}における影響の方がより顕著であった．以上より，E^{BAB} は TCR シグナル依存的に *Bim* を制御することで，ネガティブセレクションに貢献していることが示された．

E^{BAB} は抹消 T 細胞及び制御性 T 細胞の恒常性に影響を及ぼさない

胸腺内で分化，成熟した T 細胞は抹消へと流出する．また，胸腺内の high affinity TCR clone の一部はネガティブセレクションを免れ，制御性 T 細胞へと分化し，抹消で過剰な免疫応答を抑制するはたらきをする．*Bim* KO マウスでは，抹消 T 細胞及び制御性 T 細胞の数が増加することが報告されている(Bouillet et al., 2002; Labi et al., 2014)．そこで我々は，ΔE^{BAB} マウスの抹消 T 細胞及び制御性 T 細胞の数を調べた．ΔE^{BAB} マウスでは，抹消 T 細胞，制御性 T 細胞いずれの数の増加もみられなかった．したがって，E^{BAB} の機能は胸腺ネガティブセレクションに特異的であることが示された．

【参考文献】

Barnden, M.J., Allison, J., Heath, W.R., and Carbone, F.R. (1998). Defective TCR expression in transgenic mice constructed using cDNA-based alpha- and beta-chain genes under the control of heterologous regulatory elements. Immunol Cell Biol *76*, 34-40.

Bouillet, P., Purton, J.F., Godfrey, D.I., Zhang, L.C., Coultas, L., Puthalakath, H., Pellegrini, M., Cory, S., Adams, J.M., and Strasser, A. (2002). BH3-only Bcl-2 family member Bim is required for apoptosis of autoreactive thymocytes. Nature *415*, 922-926.

Calo, E., and Wysocka, J. (2013). Modification of enhancer chromatin: what, how, and why? Mol

Cell *49*, 825-837.

Klein, L., Kyewski, B., Allen, P.M., and Hogquist, K.A. (2014). Positive and negative selection of the T cell repertoire: what thymocytes see (and don't see). Nat Rev Immunol *14*, 377-391.

Labi, V., Woess, C., Tuzlak, S., Erlacher, M., Bouillet, P., Strasser, A., Tzankov, A., and Villunger, A. (2014). Deregulated cell death and lymphocyte homeostasis cause premature lethality in mice lacking the BH3-only proteins Bim and Bmf. Blood *123*, 2652-2662.

謝辞

本研究を遂行し，学位論文をまとめるにあたり，多くの方々から様々なご支援，ご指導を賜りました．

指導教員である東京大学 新領域創成科学研究科 鈴木穣教授に厚く御礼申し上げます．いつも私の研究が滞りなく進むことを最優先にご支援，ご指導いただきましたこと，大変感謝しております．共同研究者である国際電気通信基礎技術研究所 佐藤匠徳特別研究所 河岡慎平主任研究員をはじめ佐藤匠徳特別研究所 所員の皆様には研究の遂行にあたり多くのご支援，ご指導を賜りました．深く感謝いたします．共同研究者である京都大学 ウイルス・再生医科学研究所 河本宏教授，増田喬子助教，長畑洋佑氏には，主にトランスジェニックマウスの作成支援，実験手技のご指導を賜りました．免疫学がご専門である先生方のご支援のおかげで，本研究は大変充実した内容となりました．厚く御礼申し上げます．

最後に，会社員を辞め，博士課程に進むという選択を心配しながらも温かく見守ってくれた両親，弟，私の博士号取得を心待ちにしてくれていた祖父母に感謝します．そして，大学院生活の良いときも悪いときも常に寄り添い，支えてくれた夫に心から感謝します．

平成 30 年 1 月　荒井未来

Appendix

Transcriptome analysis reveals a role for the endothelial ANP-GC-A signaling in interfering with pre-metastatic niche formation by solid cancers

Introduction

Solid cancer is not a simple local disease but systemically interacts with host environment such as blood vessels, ultimately metastasizing to form secondary cancers (McAllister and Weinberg, 2014; Paget, 1989; Psaila and Lyden, 2009; Steeg, 2016). Pre-metastatic niche is one of well-known primary cancer's ability to rewire host tissues: primary cancer alters the condition of distant organs to be more preferable landing sites for disseminated cancer cells (McAllister and Weinberg, 2014; Paget, 1989; Psaila and Lyden, 2009; Steeg, 2016). A number of studies showed that the pre-metastatic niche and innate immune responses share genetic factors, suggesting that these two phenomena are closely interacting with each other (Costa-Silva et al., 2015; Hiratsuka et al., 2013; Hiratsuka et al., 2002; Hiratsuka et al., 2006; Hoshino et al., 2015; Liu et al., 2016; McAllister and Weinberg, 2014; Paget, 1989; Psaila and Lyden, 2009; Steele et al., 2016).

Atrial natriuretic peptide (ANP) is an endogenous hormone that is primarily expressed from atrial cells in the heart (Kangawa and Matsuo, 1984). Major biological roles of ANP

include promotion of diuresis, reduction of central blood pressure and inhibition of cardiac hypertrophy (Kishimoto et al., 2009). The receptor for ANP was identified in 2002: guanylyl cyclase-A (GC-A) (Li et al., 2002). There are a couple of studies suggesting a role for ANP in preventing diseases. One example is that ANP treatment may reduce the frequency of post-operative lung cancer-recurrence in lung cancer patients post-surgery (Nojiri et al., 2015). The same study also uncovered that ANP inhibits cancer metastasis in the mouse model of solid cancers such as F16/F10 melanoma (Nojiri et al., 2015). To extend clinical applications of ANP, and to use ANP for preventing cancer recurrence, it is essential to investigate whether these observations can be extended to other solid cancers. It is also important to understand how ANP prevents cancer metastasis, particularly, which metastatic step(s) ANP interferes with.

Here, in collaboration with Dr. Kangawa's group, the one who identified ANP, I tried answer the above-described questions. I found that the ANP-GC-A pathway inhibits pre-metastatic niche formation in two different solid cancer models, indicating a general role for ANP in metastasis suppression. Comprehensive gene expression analyses I performed revealed that ANP treatment significantly suppressed gene expression changes caused by cancer transplantation, which represent pre-metastatic niche formation in the lung. Additionally, I was able to find extensive similarities between ANP treatment and GC-A overexpression in endothelial cells on antagonizing cancer-induced gene expression changes. GC-A

experiments were in particular important to demonstrate that endothelial cells mediate ANP-dependent inhibition of the pre-metastatic niche.

Results and Discussion

In the study, I performed transcriptome analyses to investigate how ANP-GC-A signaling prevents cancer metastasis. Data provided by Dr. Kangawa's group was basis for my analyses. Hence, I briefly summarize the data provided: in vivo assessment on effects of ANP treatment on cancer metastasis. To quantify the effect of ANP on cancer metastasis, a transplantation model of mouse breast cancer 4T1 (EGFP) (4T1-EGFP) was used. 1st recipient BALB/c mice used for obtaining cancer tissues, which was transplanted into the mammary pad of 2nd recipient. Mice were further sacrificed at 28 dpt .The results showed that ANP-treatment significantly reduced the number of GFP-positive metastases to the lungs, one of the most frequent targets for metastasis (Figure 1, Figure 2). Neither volume nor weight of primary 4T1 tumor was significantly affected by ANP treatment (Figure 3, Figure 4). Thus, it was likely that ANP prevents metastasis of 4T1 cancer to the lungs, and importantly, seemingly does not affect the nature (e.g. survival) of cancer cells.

To know how ANP accomplished its anti-metastasis activity, I investigated the effects of ANP on lung gene expression with or without 4T1 transplantation via RNA-seq. The lungs

from control and 4T1-bearing mice treated with vehicle or ANP (thus four experimental groups) were subjected to gene expression analyses at 7 dpt, roughly 2 weeks before visible metastases are detected. I found that, in the lung of 4T1-bearing mice in comparison to those of controls, genes associated with inflammation were prominently elevated (Figure 5). Gene ontology analyses in fact validated that the up-regulated genes were indicative of increases in "leukocyte migration", "neutrophil chemotaxis", and "myeloid leukocyte migration" (Figure 6). Notably, ANP suppressed most of 4T1-induced gene expression changes in the lungs of 4T1-bearing mice (Figure 7, Figure 8) while unaffected expression of 4T1-induced genes in the normal lung (Figure 8). These indicated that ANP inhibit pre-metastatic niche formation—inflammation—in the lung in 4T1-bearing mice.

Next, to extend the above-described observation, the inhibitory activity of ANP against pre-metastatic niche formation was tested in the Lewis Lung Carcinoma-EGFP (LLC-EGFP) model using C57BL/6 male mice. I analyzed lung gene expression at 10 dpt and found that, as was the case for the lungs in the 4T1 model, expression of inflammation markers was elevated in the lung of LLC-bearing mice. I decided to analyze the lungs at 10 dpt simply because LLC-EGFP model grows less aggressively. Gene set enrichment analyses (GSEA) demonstrated that up-regulated genes in 4T1-bearing mice were strikingly similar to those in LLC-bearing mice (Figure 9). Importantly, similar to the 4T1 model (Figure 7, Figure 8), ANP canceled gene

expression changes caused by LLC in the lung (Figure 10, Figure 11). Moreover, the lungs of C57BL/6 males appeared to be largely unresponsive to ANP at the mRNA level in the absence of LLC (Figure 11). Taking the results from two solid cancer models together, I concluded that ANP's role in suppressing cancer-induced gene expression changes might be generalizable, and that the activity was specific to cancer-bearing condition.

ANP exerts its biological roles via interaction with a receptor called guanylyl cyclase-A (GC-A) (Li et al., 2002). Mice overexpressing *GC-A* specifically in endothelial cells (termed EC GC-A-Tg mice) were utilized to address whether this can mimick ANP treatment (Kishimoto et al., 2009; Li et al., 2002; Nojiri et al., 2015). It is known that overexpression of GC-A in endothelial cells can activate ANP-GC-A signaling. Littermate mice with or without *GC-A* overexpression in endothelial cells were given LLC cancer tissues, and then sacrificed at 10 dpt for RNA-seq analyses. I found that the extent of LLC-induced gene upregulations were suppressed in the lung of EC GC-A-Tg compared to the littermate controls (Figure 12, Figure 13). Interestingly, EC GC-A-Tg had only a minor effect on lung gene expression in the absence of cancer tissues (Figures 13), which was reminiscent to observations in ANP administration experiments. Yet, extensive similarities (> 95%) were found between ANP-suppressed genes and EC GC-A Tg-affected genes in the LLC-bearing mice. These results suggest that ANP inhibited pre-metastatic niche formation through endothelial *GC-A* (Figure 14).

In summary, I concluded that endothelial ANP-GC-A signaling inhibits pre-metastatic niche formation in 4T1 and LLC bearing mice but does not affect the lung in cancer-free mice. I propose this pathway could be a target for drugging pre-metastatic niches by solid cancers (Nojiri et al., 2017).

Figures

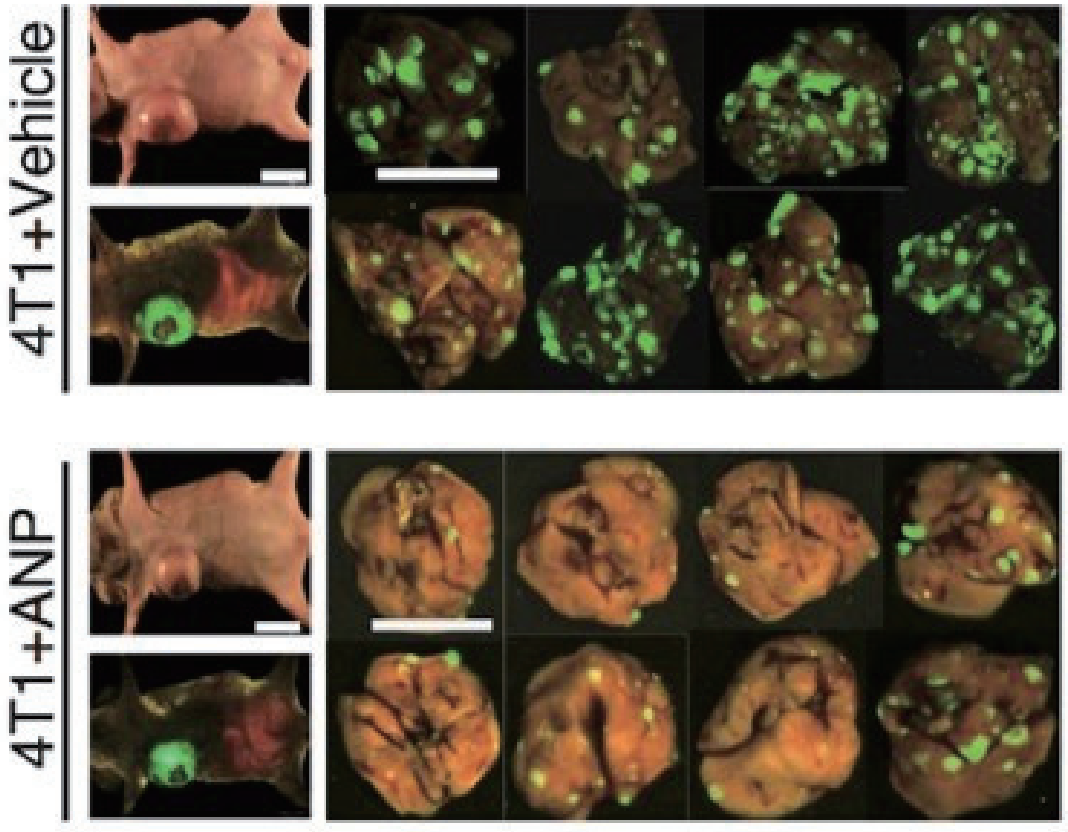

Figure 1 Representative images of lung metastasis in vehicle- or ANP-treated 4T1-bearing mice.

Mice were sacrificed four weeks after cancer cell transplantation. Scale bars represent 10 mm.

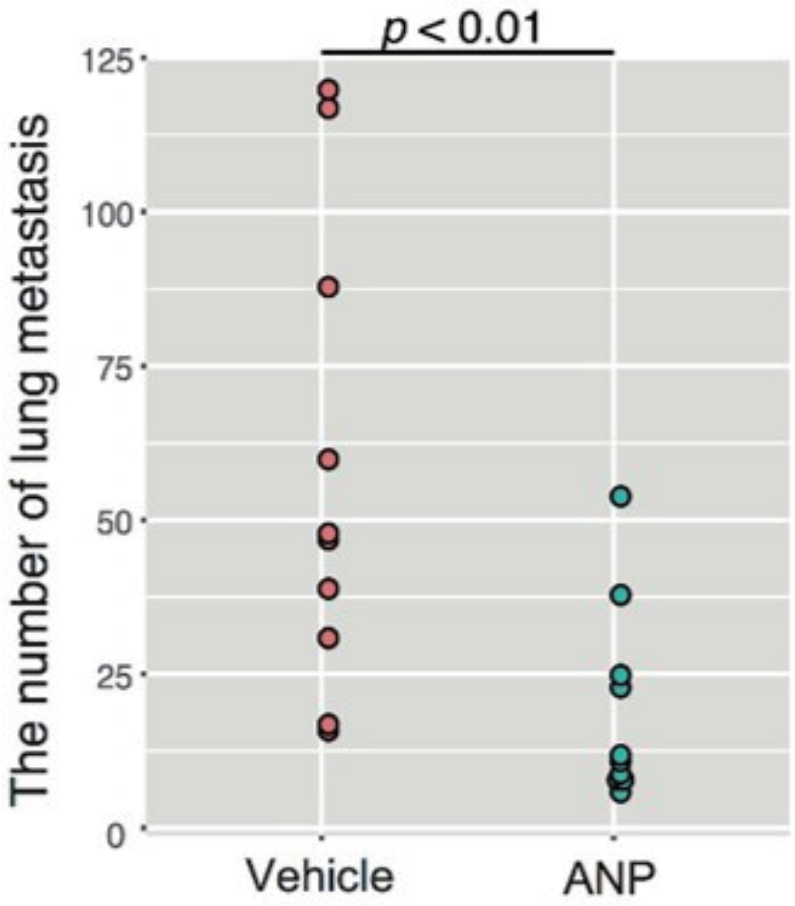

Figure 2 Dot plot showing the number of nodules representing lung metastasis of 4T1-EGFP cells in mice grouped as in Figure 1 (10 mice per a group).

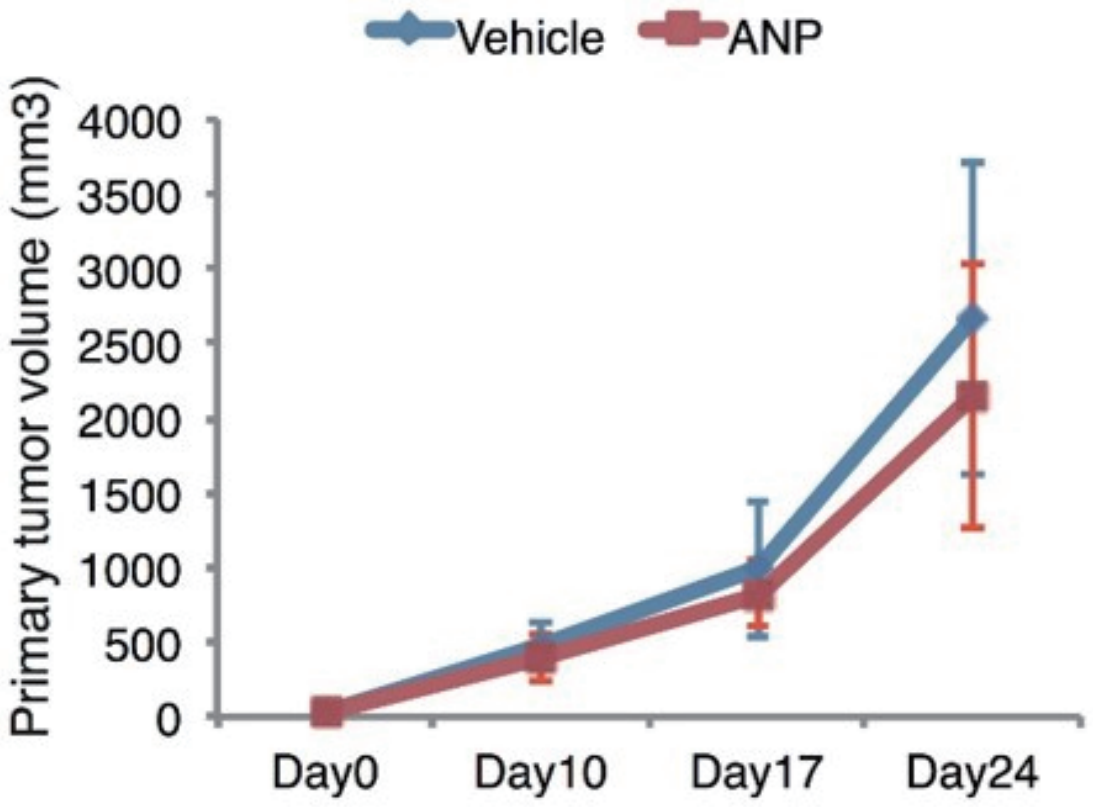

Figure 3 Primary tumor volume in vehicle- or ANP-treated 4T1-bearing mice on day 10, 17, and 24 after cancer cell transplantation. Data are means ± s.e.m. (10 mice per a group).

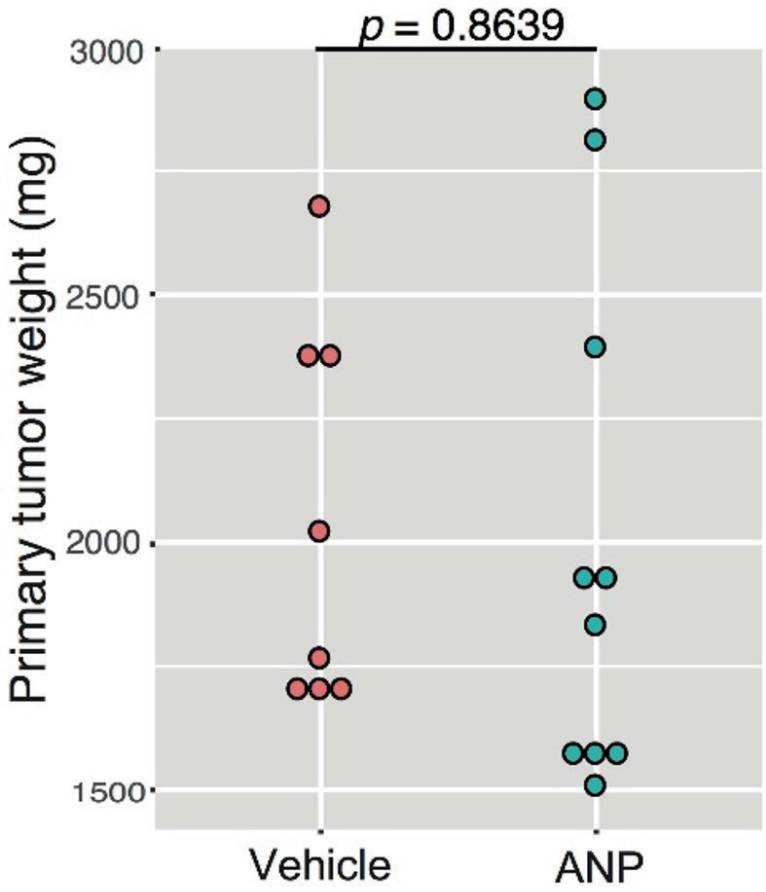

Figure 4 Primary tumor weight in vehicle- or ANP-treated 4T1-bearing mice on 28 dpt (9 mice for vehicle and 8 for ANP).

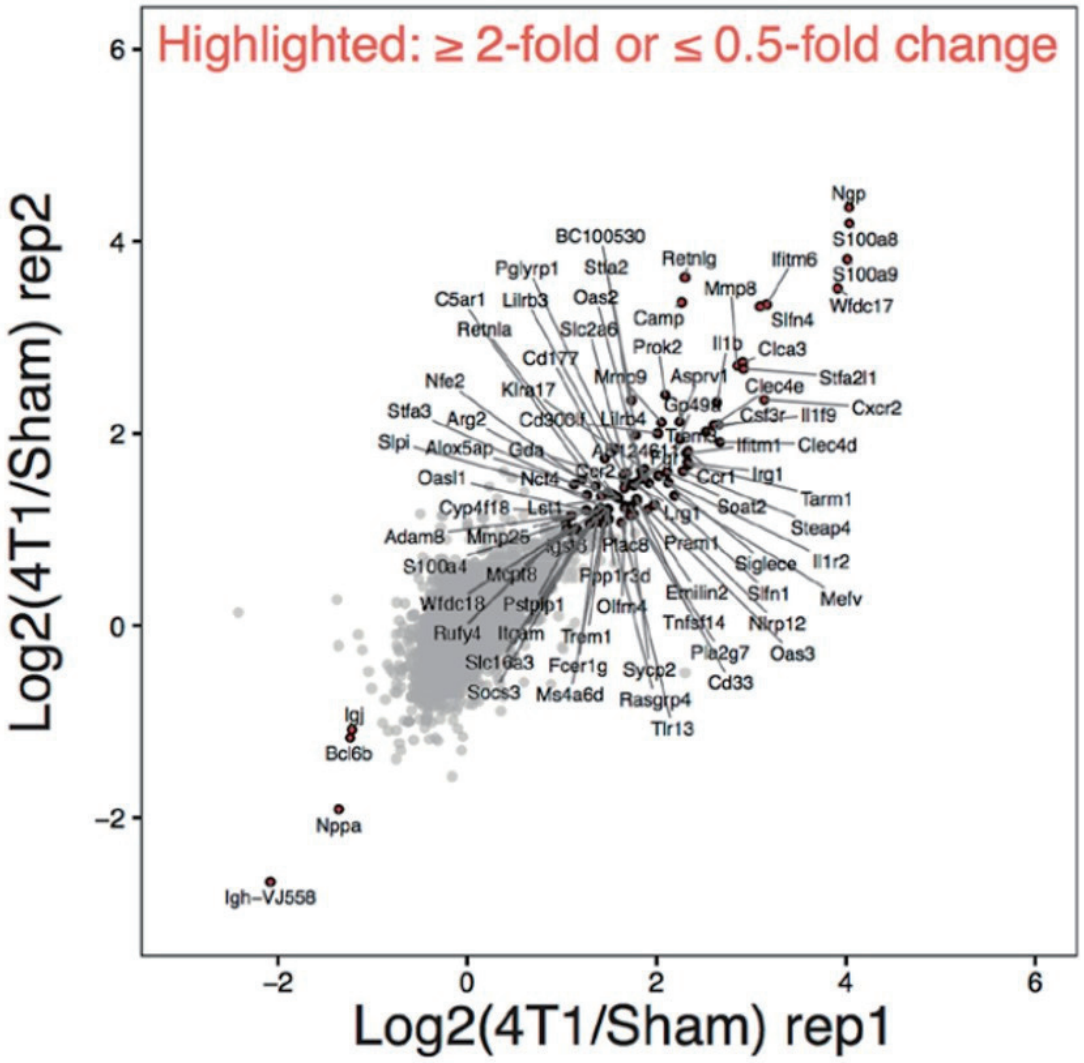

Figure 5 Scatter plot showing log2 fold changes between the lungs of 4T1-bearing or sham-operated mice. Genes exhibiting more than 2-fold changes are highlighted. Data from two biological replicates are shown (rep1 and rep2).

Gene ontology	Fold enrichment	*p*-value
Fc-gamma receptor signaling pathway (GO:0038094)	> 100	6.88E-03
leukocyte migration involved in inflammatory response (GO:0002523)	80.53	5.10E-05
neutrophil chemotaxis (GO:0030593)	38.22	1.62E-09
neutrophil migration (GO:1990266)	35.79	3.07E-09
granulocyte chemotaxis (GO:0071621)	34.69	4.16E-09
granulocyte migration (GO:0097530)	32.21	8.58E-09
leukocyte chemotaxis (GO:0030595)	30.65	4.03E-13
myeloid leukocyte migration (GO:0097529)	30.06	9.52E-11
leukocyte migration (GO:0050900)	24.57	5.60E-15

Figure 6 Gene ontology analysis. Top 100 up-regulated genes were subjected to GO analysis and signatures highly significantly enriched in the group are shown.

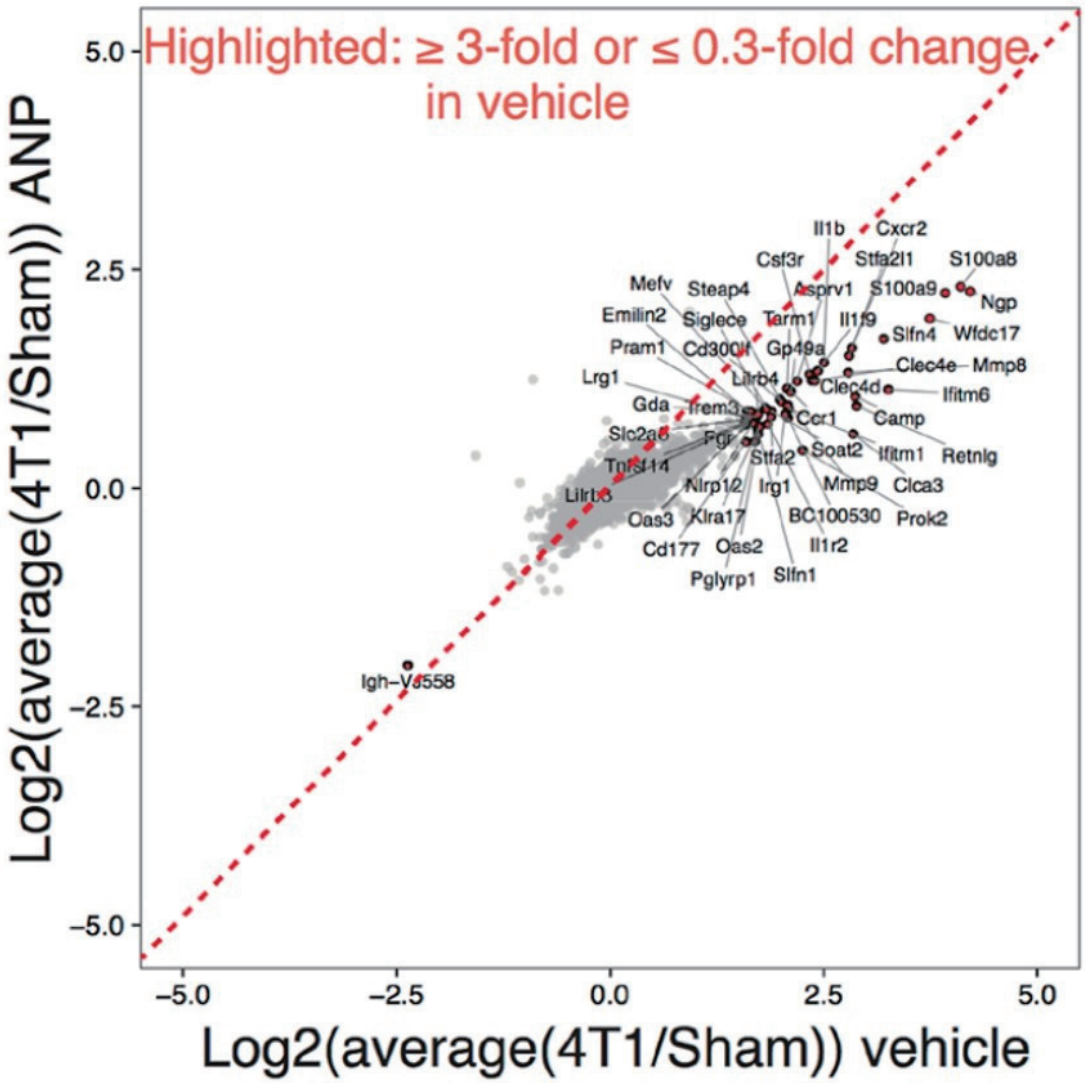

Figure 7 Scatter plot comparing log2 fold changes between 4T1-bearing or sham-operated mice with or without ANP treatment. Genes exhibiting ≥ 3-fold or ≤ 0.3-fold changes in vehicle are highlighted. Data from two biological replicates are averaged.

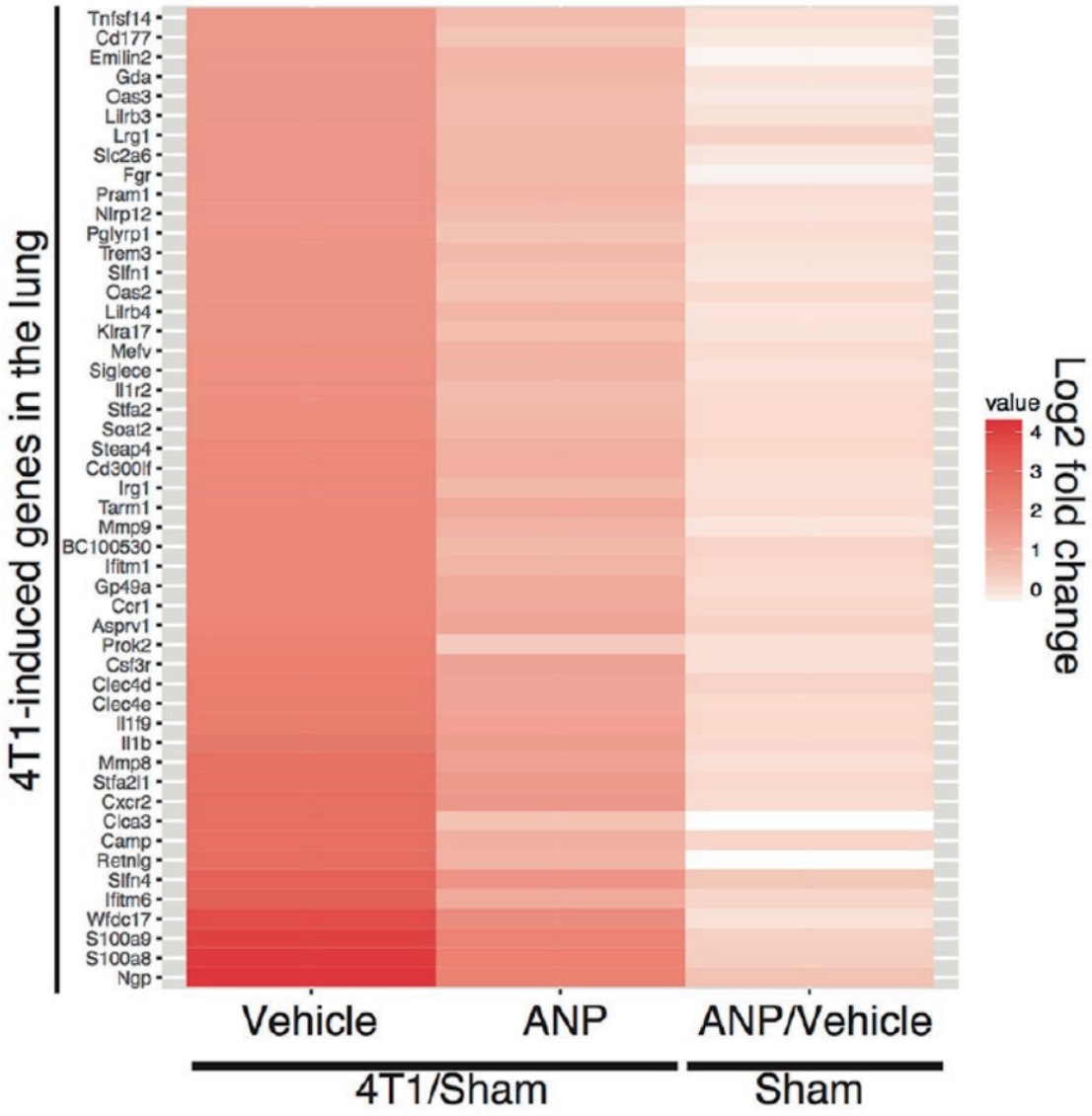

Figure 8 Heatmap of genes exhibiting more than 3-fold increases in the lung of 4T1-bearing mice is shown. Gene expression changes of the indicated genes in ANP-treated sham group are also shown.

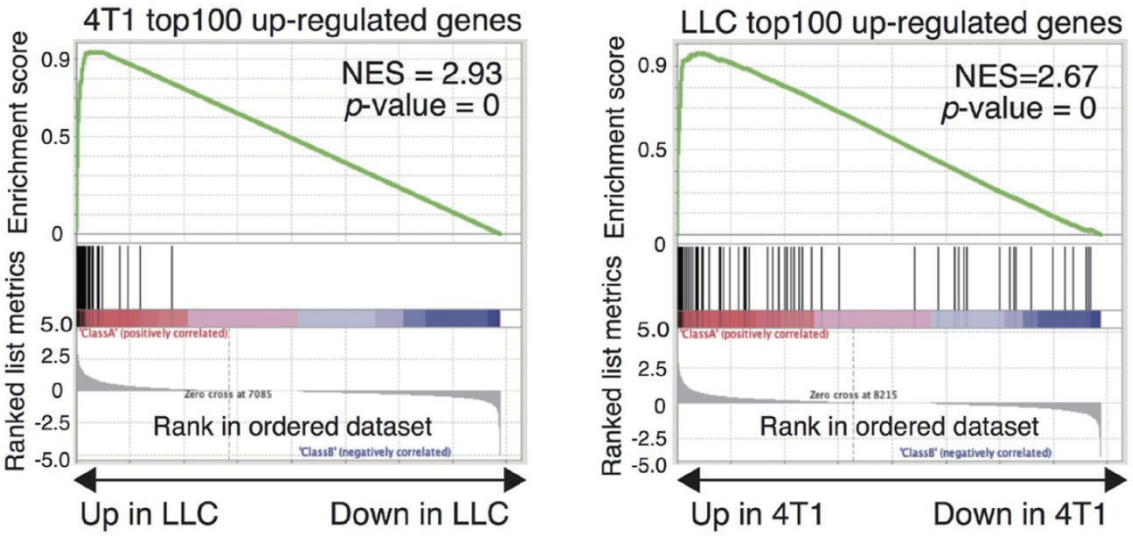

Figure 9 Gene set enrichment analysis comparing 4T1- and LLC-induced gene expression changes in the lung.

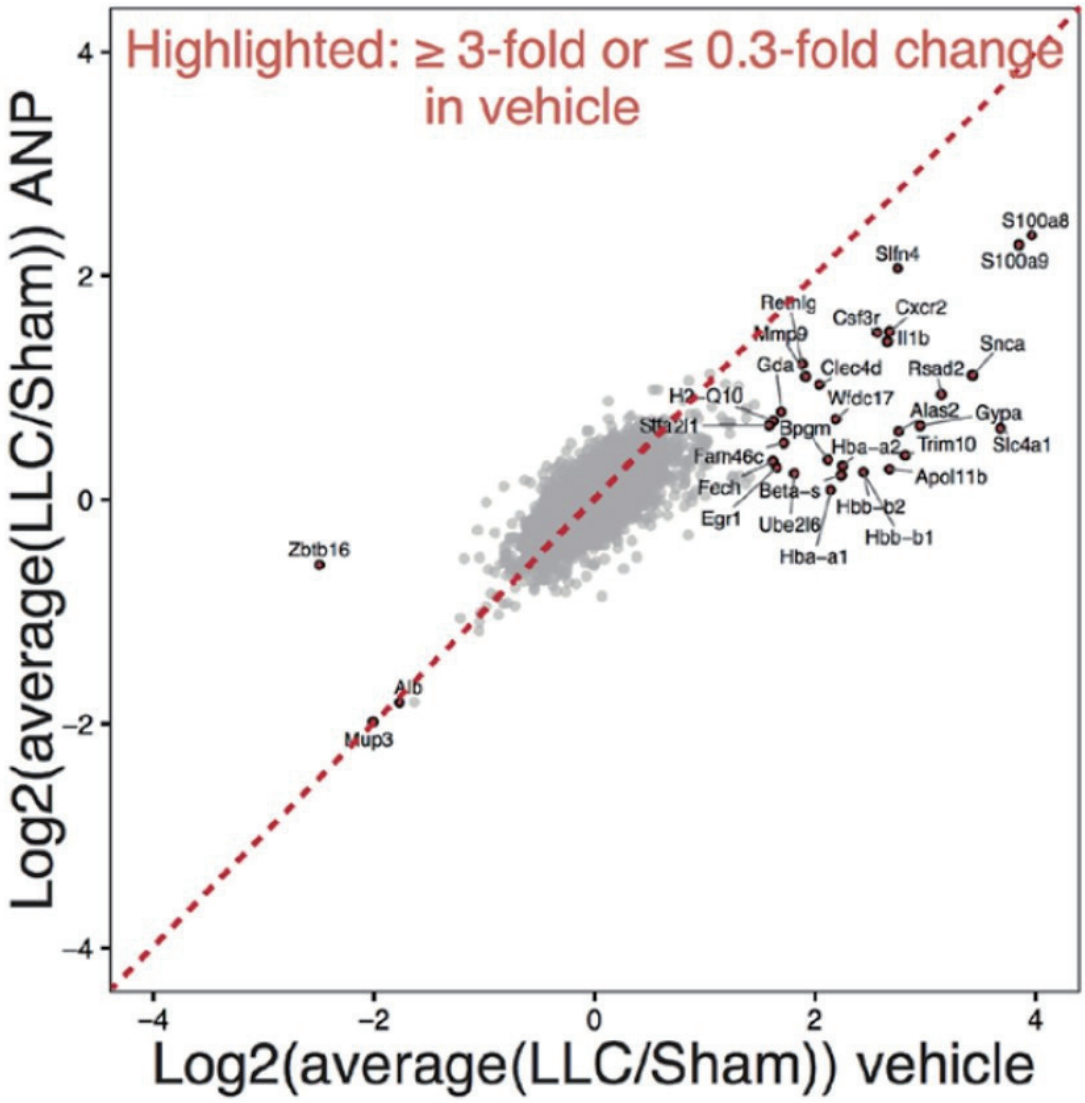

Figure 10 Scatter plot comparing log2 fold changes between LLC-bearing or sham-operated mice with or without ANP treatment. Genes exhibiting ≥ 3-fold or ≤ 0.3-fold changes in vehicle are highlighted. Data from two biological replicates are averaged.

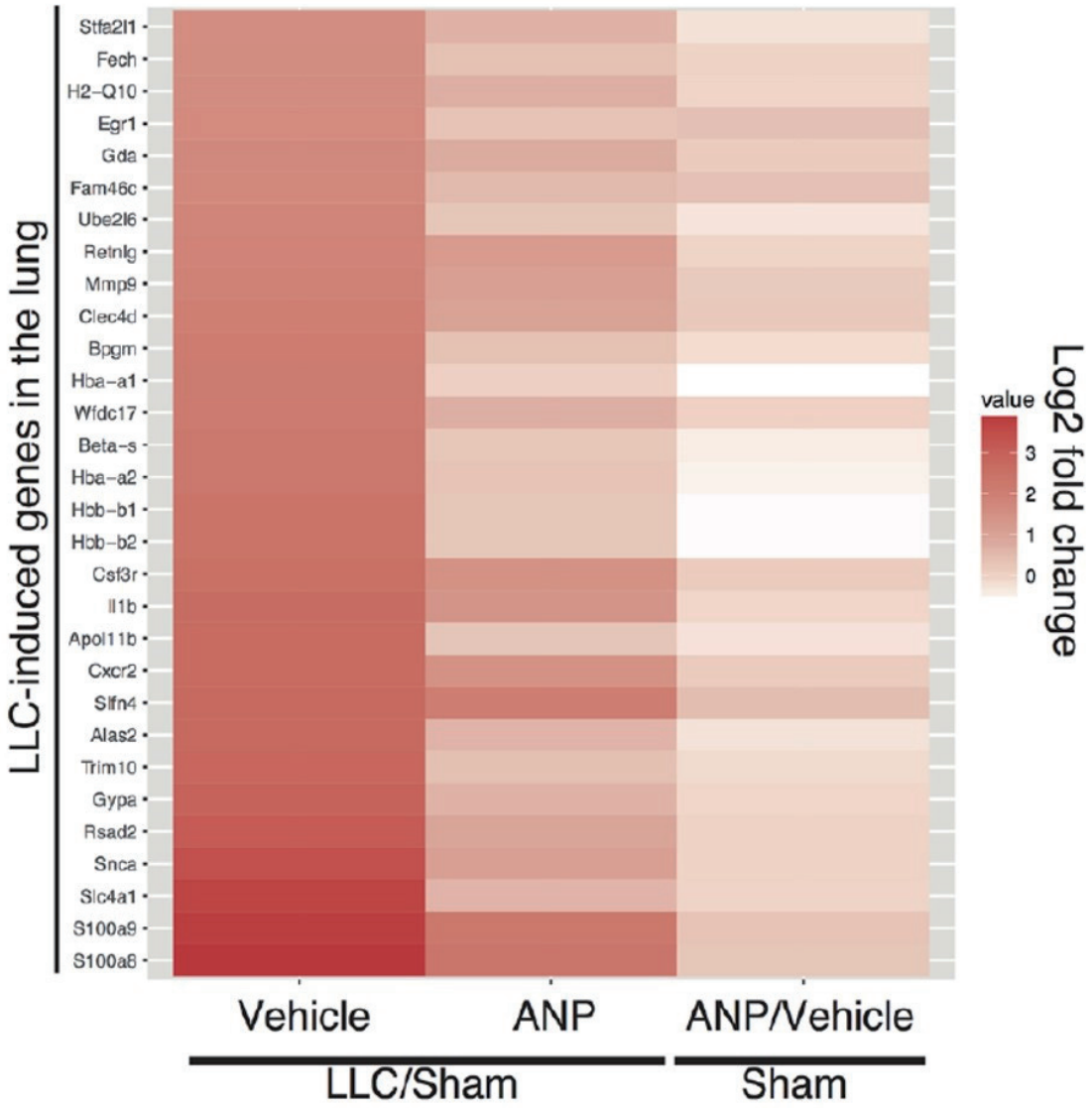

Figure 11 Heatmap of genes exhibiting more than 3-fold increases in the lung of LLC-bearing mice is shown. Gene expression changes of the indicated genes in the ANP-treated sham group are also shown.

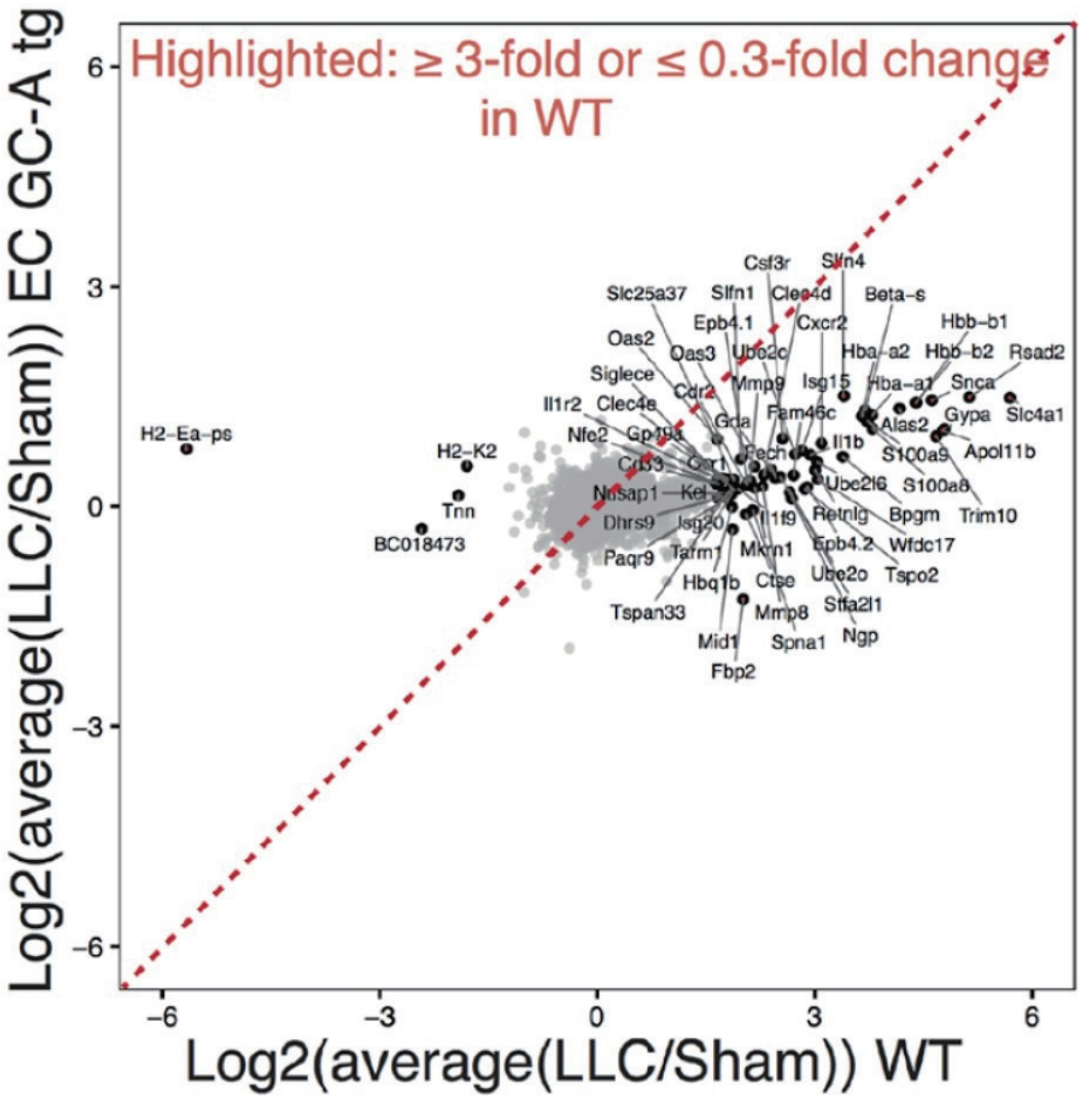

Figure 12 Scatter plot comparing log2 fold changes between LLC-bearing or sham-operated mice in WT and EC GC-A-Tg. Genes exhibiting ≥ 3-fold or ≤ 0.3-fold changes are highlighted. Data from two biological replicates are averaged.

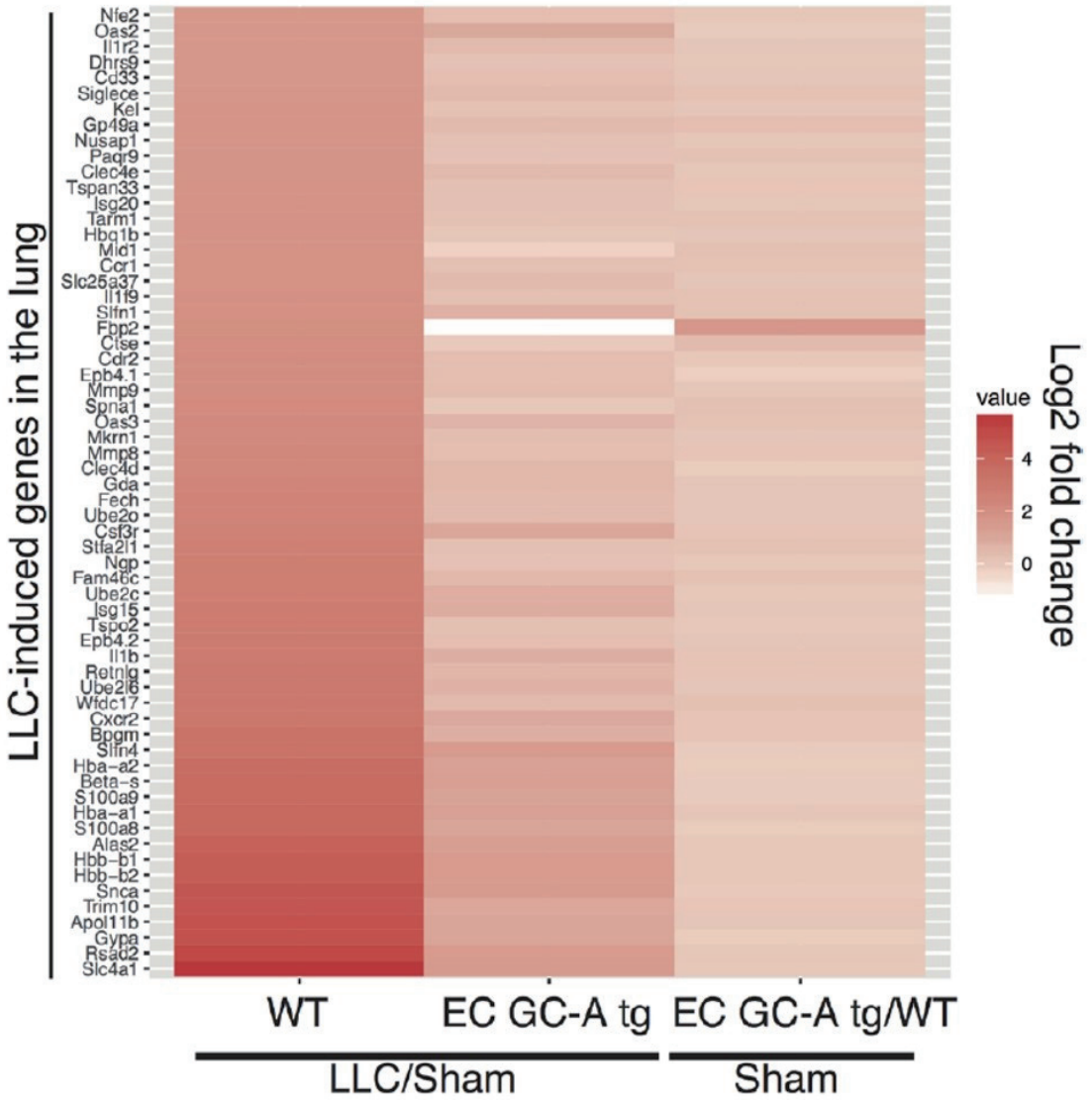

Figure 13 Heatmap of genes exhibiting more than 3-fold increases in the lung of LLC-bearing WT mice is shown. Gene expression changes of the indicated genes between WT and EC GC-A-Tg (sham-operated) are also shown.

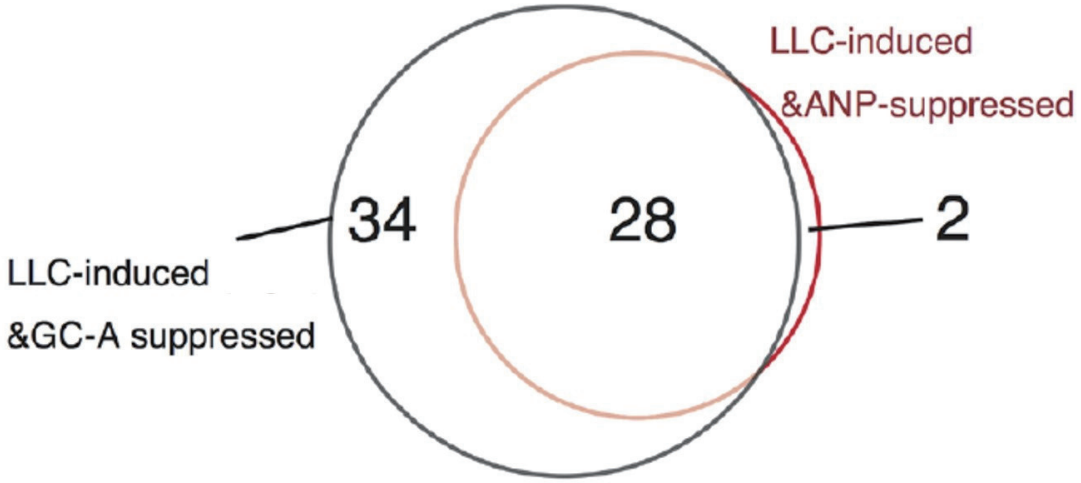

Figure 14 Venn diagram demonstrates extensive overlap between ANP- or GC-A-regulated genes.

References

Costa-Silva, B., Aiello, N.M., Ocean, A.J., Singh, S., Zhang, H., Thakur, B.K., Becker, A., Hoshino, A., Mark, M.T., Molina, H.*, et al.* (2015). Pancreatic cancer exosomes initiate pre-metastatic niche formation in the liver. Nat Cell Biol *17*, 816-826.

Hiratsuka, S., Ishibashi, S., Tomita, T., Watanabe, A., Akashi-Takamura, S., Murakami, M., Kijima, H., Miyake, K., Aburatani, H., and Maru, Y. (2013). Primary tumours modulate innate immune signalling to create pre-metastatic vascular hyperpermeability foci. Nat Commun *4*, 1853.

Hiratsuka, S., Nakamura, K., Iwai, S., Murakami, M., Itoh, T., Kijima, H., Shipley, J.M., Senior, R.M., and Shibuya, M. (2002). MMP9 induction by vascular endothelial growth factor receptor-1 is involved in lung-specific metastasis. Cancer Cell *2*, 289-300.

Hiratsuka, S., Watanabe, A., Aburatani, H., and Maru, Y. (2006). Tumour-mediated upregulation of chemoattractants and recruitment of myeloid cells predetermines lung metastasis. Nat Cell Biol *8*, 1369-1375.

Hoshino, A., Costa-Silva, B., Shen, T.L., Rodrigues, G., Hashimoto, A., Tesic Mark, M., Molina, H., Kohsaka, S., Di Giannatale, A., Ceder, S.*, et al.* (2015). Tumour exosome integrins determine organotropic metastasis. Nature *527*, 329-335.

Kangawa, K., and Matsuo, H. (1984). Purification and complete amino acid sequence of

alpha-human atrial natriuretic polypeptide (alpha-hANP). Biochem Biophys Res Commun *118*, 131-139.

Kishimoto, I., Tokudome, T., Horio, T., Garbers, D.L., Nakao, K., and Kangawa, K. (2009). Natriuretic Peptide Signaling via Guanylyl Cyclase (GC)-A: An Endogenous Protective Mechanism of the Heart. Curr Cardiol Rev *5*, 45-51.

Li, Y., Kishimoto, I., Saito, Y., Harada, M., Kuwahara, K., Izumi, T., Takahashi, N., Kawakami, R., Tanimoto, K., Nakagawa, Y.*, et al.* (2002). Guanylyl cyclase-A inhibits angiotensin II type 1A receptor-mediated cardiac remodeling, an endogenous protective mechanism in the heart. Circulation *106*, 1722-1728.

Liu, Y., Gu, Y., Han, Y., Zhang, Q., Jiang, Z., Zhang, X., Huang, B., Xu, X., Zheng, J., and Cao, X. (2016). Tumor Exosomal RNAs Promote Lung Pre-metastatic Niche Formation by Activating Alveolar Epithelial TLR3 to Recruit Neutrophils. Cancer Cell *30*, 243-256.

McAllister, S.S., and Weinberg, R.A. (2014). The tumour-induced systemic environment as a critical regulator of cancer progression and metastasis. Nat Cell Biol *16*, 717-727.

Nojiri, T., Arai, M., Suzuki, Y., Kumazoe, M., Tokudome, T., Miura, K., Hino, J., Hosoda, H., Miyazato, M., Okumura, M.*, et al.* (2017). Transcriptome analysis reveals a role for the endothelial ANP-GC-A signaling in interfering with pre-metastatic niche formation by solid cancers. Oncotarget *8*, 65534-65547.

Nojiri, T., Hosoda, H., Tokudome, T., Miura, K., Ishikane, S., Otani, K., Kishimoto, I., Shintani, Y., Inoue, M., Kimura, T.*, et al.* (2015). Atrial natriuretic peptide prevents cancer metastasis through vascular endothelial cells. Proc Natl Acad Sci U S A *112*, 4086-4091.

Paget, S. (1989). The distribution of secondary growths in cancer of the breast. 1889. Cancer Metastasis Rev *8*, 98-101.

Psaila, B., and Lyden, D. (2009). The metastatic niche: adapting the foreign soil. Nat Rev Cancer *9*, 285-293.

Steeg, P.S. (2016). Targeting metastasis. Nat Rev Cancer *16*, 201-218.

Steele, C.W., Karim, S.A., Leach, J.D., Bailey, P., Upstill-Goddard, R., Rishi, L., Foth, M., Bryson, S., McDaid, K., Wilson, Z.*, et al.* (2016). CXCR2 Inhibition Profoundly Suppresses Metastases and Augments Immunotherapy in Pancreatic Ductal Adenocarcinoma. Cancer Cell *29*, 832-845.